

Supplementary Material from Ziburkus J, Cressman JR, Barreto E, and Schiff SJ, Interneuron and pyramidal cell interplay during in vitro seizure-like events, Journal of Neurophysiology, 95: 3948-3954, 2006.

Supplementary Methods.

Electrophysiology. Simultaneous dual and triple whole-cell and extracellular (DC mode) recordings were performed in the CA1 area of hippocampus. Putative oriens interneurons were distinguished from excitatory pyramidal cells using these criteria: 1) horizontal appearance and location of cell bodies using differential infrared contrast microscopy (Zeiss Axioskop), 2) membrane resting potential (pyramidals: $V_{m_{rest}} = -67 \pm 0.8$ mV, $n=40$; interneurons: $V_{m_{rest}} = -62 \pm 1$ mV, $n=15$), 3) active membrane properties: spike height (pyramidals: 80 ± 5.2 mV; interneurons: 68 ± 2.9 mV) and spike width at half-height (pyramidals: 1.4 ± 0.1 msec; interneurons: 1.1 ± 0.2 msec) (Fig. 2A), and 4) post-hoc morphological analysis using biocytin histochemistry (Fig.2B). To describe dominant currents and spike trains, the cells were held at -75 mV and incremental (50 - 100 pA; 500 msec) negative and positive square wave current pulses were injected (Fig 2A). Oriens lacunosum moleculare interneurons, following negative current pulses, exhibit a characteristic initial hyperpolarizing sag, an inward rectification, and triangularly shaped afterhyperpolarizations as seen in Fig 2A (Maccaferri and McBain 1996; Maccaferri and Lacaille 2003). For the entire duration of the experiments, the cells were held with bias currents no greater than -100 pA. Only cells with input resistance greater than 100 M Ω and access resistance of less than 20 M Ω were included in the final analysis.

Histochemistry. Neurons filled with neurobiotin were processed using the modified biocytin histological methods of Horikawa and Armstrong (1988). In brief, 350 μ M sections were placed in 4% paraformaldehyde overnight. After rinsing in phosphate

buffered saline (PBS) and incubation in 10% methanol and 0.15% hydrogen peroxide overnight at 4°C, slices were reacted with 1% avidin-biotin complex (ABC Elite Kit, Vector Laboratories), 1.8% NaCl, and 0.5% Triton X-100 in PBS) overnight at 4°C. Slices were then rinsed in PBS and 0.1M acetate buffer (pH 6.0) and reacted with diaminobenzidine and glucose oxidase in PBS using nickel ammonium sulfate intensification (5-15 min). The reaction was stopped with the acetate buffer. In our hands, most of the histochemically processed cells did not reveal complete axonal staining and the final putative classification of interneurons was based on their somatic location, dendritic morphology, and membrane firing properties. To detail the dendritic morphology of the filled cells, camera lucida drawings and photographs were taken with an Olympus microscope.

Gap junction blockade. To block gap junctions, 2-100 μ M bath application of carbenoxolone was used. Carbenoxolone (Sigma) was dissolved in saline and diluted in the ACSF.

Correlation Analysis. For spike correlation, a simple threshold was used initially to identify spike times. The times of spike initiation and termination were determined by measuring the slope of the membrane potential over a fraction of a millisecond. The slope threshold for spike initiation was set to a finite positive value, typically 25 mV/msec. The end slope was chosen to be zero, thus forcing the spike to end before any subsequent spikes would begin.

For subthreshold voltages, correlations were calculated within non-overlapping sliding time windows of 1 second. The continuous crosscorrelation function, $c_{i,j}(\tau)$, for each pair of neurons i and j for each time window T was calculated using:

$$c_{i,j}(\tau) = \frac{\sum_{t=-T/2}^{T/2} x_i(t)x_j(t+\tau)}{\left(\sum_{t=-T/2}^{T/2} (x_i(t))^2\right)^{1/2} \left(\sum_{t=-T/2}^{T/2} (x_j(t))^2\right)^{1/2}}, \text{ where } x(t) \text{ is the voltage (with mean}$$

removed) at time t for channel i or j , and τ is the time lag.

The absolute value of $c_{i,j}(\tau)$ at each time lag was compared to the Bartlett estimator of crosscorrelation standard error, $\sigma_{i,j}$, (Bartlett 1946; Box and Jenkins 1976):

$$\sigma_{i,j}^2(\tau) = \left| \frac{\sum_{\tau=-T/2}^{T/2} c_{i,i}(\tau)c_{j,j}(\tau)}{(T+1-\tau)} \right|, \text{ determined from the autocorrelation functions of each}$$

signal, $c_{i,i}(\tau)$, $c_{j,j}(\tau)$, where $|\cdot|$ indicates absolute value. The correlation value for each window was then determined by the sum, S , of the crosscorrelation values greater than

two times the standard error: $S = \sum_{\tau=-T/2}^{T/2} |c_{i,j}(\tau)| \theta(|c_{i,j}(\tau)| - 2\sigma_{i,j}(\tau))$, where θ is the

Heaviside function (1 if $|c_{i,j}(\tau)| - 2\sigma_{i,j}(\tau) > 0$, and 0 otherwise). This method reduces the spurious crosscorrelation effects due to the magnitude of the autocorrelation of the individual signals and takes into account the finite nature of the short time series used.

For spikes, we binned the time series of spikes, $s(t)$, for each pair of neurons i and j , by discretizing time into N intervals of 10 milliseconds. The point process correlation, $p_{i,j}(\tau)$, corrected for the expected product of the spike numbers n , m within $-T/2 < t < T/2$ for

neuron i and j respectively, is $p_{i,j}(\tau) = \frac{1}{nm} \left[\sum_{t=-T/2}^{T/2} s_i(t)s_j(t+\tau) - \frac{nm}{N} \right]$ (Brody, 1991). The

spike rate correction compensates for the effects of increased correlations due to increased activity. As stated above, correlations in the individual signals can erroneously produce higher correlation values in the cross correlation signal. In order to account for

this effect, we once again used a Bartlett estimator to determine the significance of $p_{i,j}(\tau)$.

The Bartlett estimator was calculated in the same manner as for the synaptic correlations,

using the autocorrelation function $g_{i,i}(\tau) = \frac{1}{n^2} \left[\sum_{t=-T/2}^{T/2} s(t)_i s(t+\tau)_i - \frac{n^2}{N} \right]$.

Supplementary Results

EI interplay during epileptiform bursts

Shortly after application of 4-AP (100 μ M) we observed burst firing in EE and EI pairs. These events were network driven, as they were also reflected in the extracellular recordings (Supplementary Fig. 1A-C). Interneurons produced more spikes than pyramidal cells and often exhibited a short (up to 100 msec) depolarization block which coincided with burst firing in pyramidal cells (Supplementary Fig. 1C,D). These findings coupled with other recent reports (Aradi and Maccaferri, 2004) show that distinct timing interplay of inhibition and excitation might also exist during *in vitro* interictal-like burst firing events.

Gap junctions and seizures

Recent findings show that electrotonic coupling is present between oriens interneurons (Zhang et al. 2004) and that gap junctions connecting putative cortical interneurons increase synchrony (Merriam et al. 2005). To test whether 4-AP seizures and DB are dependent on gap junction connectivity, we bath applied low concentrations (2-20 μ M) of carbenoxolone to cells exhibiting seizures (Supplementary Fig. 2, n=4 interneurons and n=4 pyramidal cells). Using these low concentrations of carbenoxolone we were able to manipulate the length of depolarization block and SLE. The length of DB in interneurons decreased with increasing concentration of carbenoxolone in increments as small as 2 μ M (Supplementary Fig. 2A). In half of the slices, SLE could be blocked

with 20 μ M carbenoxolone. However, in some cases to completely block SLE and neuronal hyperexcitability, higher carbenoxolone concentrations were needed (20-100 μ M; n=4). Following wash out of carbenoxolone (~1 hour, n=2), DB and recurring seizures (of shorter duration) returned. Thus, electrotonic coupling may play a role in the sequence of the EI interplay that we have here described.

The full spectrum of the effects of carbenoxolone is under scrutiny. In rat hippocampal glial-neuronal cocultures where only glial cells were electrotonically coupled, high concentrations (100 μ M) of carbenoxolone could directly affect neuronal excitability (Rouach et al., 2003). On the other hand, experiments in *in vitro* slice and intact hippocampal preparations showed minimal effects of carbenoxolone on intrinsic neuronal membrane properties (100-150 μ M) and a potent effect on electrotonic coupling between O-LM cells (Yang and Michelson 2001; Zhang et al. 2004). We observed distinct effects with concentrations as low as 2 μ M, and a clear concentration dependency between 2-20 μ M. Although further experiments with more specific neuronal gap junction blockers and recordings from electrically coupled cells will be required to more definitively establish the role of gap junctions in SLE, our results are highly suggestive that gap junction connectivity plays a role in DB and SLE.

Supplementary References:

Aradi I, Maccaferri G. Cell type-specific synaptic dynamics of synchronized bursting in the juvenile CA3 rat hippocampus. *J Neurosci* 24:9681-92, 2004.

Bartlett MS. On the theoretical specification of sampling properties of autocorrelated time series. *J Royal Stat Soc B8*, 27, 1946.

Box GE and Jenkins GM. *Time series analysis forecasting and control*. Holden-Day, California, 1976.

Brody CD. Correlations without synchrony. *Neural Comput*, 11:1537-1551, 1991.

Horikawa K and Armstrong WE. A versatile means of intracellular labeling: injection of biocytin and its detection with avidin conjugates. *J Neurosci Methods* 25:1-11, 1988.

Maccaferri G and McBain CJ. The hyperpolarization-activated current (I_h) and its contribution to pacemaker activity in rat CA1 hippocampal stratum oriens-alveus interneurons. *J Physiol* 497:119-130, 1996.

Maccaferri G and Lacaille JC. Interneuron Diversity series: Hippocampal interneuron classifications - making things as simple as possible, not simpler. *Trends Neurosci* 26:564-71, 2003.

Merriam EB, Netoff TI and Banks MI. Bistable network behavior of layer I interneurons in auditory cortex. *J Neurosci* 25:6175-86, 2005.

Rouach N, Segal M, Koulakoff A, Giaume C and Avignone E. Carbenoxolone blockade of neuronal network activity in culture is not mediated by an action on gap junctions. *J Physiol*. 553:729-45, 2003.

Yang Q and Michelson HB. Gap junctions synchronize the firing of inhibitory interneurons in guinea pig hippocampus. *Brain Res* 907:139-43, 2001.

Zhang X-L, Zhang L, and Carlen PL. Electrotonic coupling between stratum oriens interneurons in the intact mouse juvenile hippocampus. *J Physiol* 558:825-839, 2004.

Supplementary Figure Legends

Supplementary Figure 1. Interneuron and pyramidal interplay during interictal

burst discharges. A. Traces of three simultaneous recordings from an interneuron (ellipse, top), pyramidal cell (triangle, middle), and extracellular electrode (EC, bottom).

B. Expanded portion of the burst discharges from A. **C.** Single burst at expanded scale

from B. **D.** Burst from a dual recording of an interneuron and pyramidal cell taken from another slice. Note that pyramidal cells fire most of their spikes in the middle of the time period of the interneuron paroxysmal depolarizing shift and burst discharge. The interneurons show a brief period of near spike inactivation in C, and a longer inactivation in D.

Figure 2. Interneurons in DB and gap junctions. A. Compressed data segment

showing three recurring DBs during seizures in an oriens interneuron. Bath application of increasing carbenoxolone (CARB) concentrations (2, 4, 6, 8, 10, 12, 14, 16, 20, and 24 μ M) decreased the duration of the DB (n=3). Inset graph (top right) shows duration of DB (ordinate) for the same interneuron from which the example traces are taken.

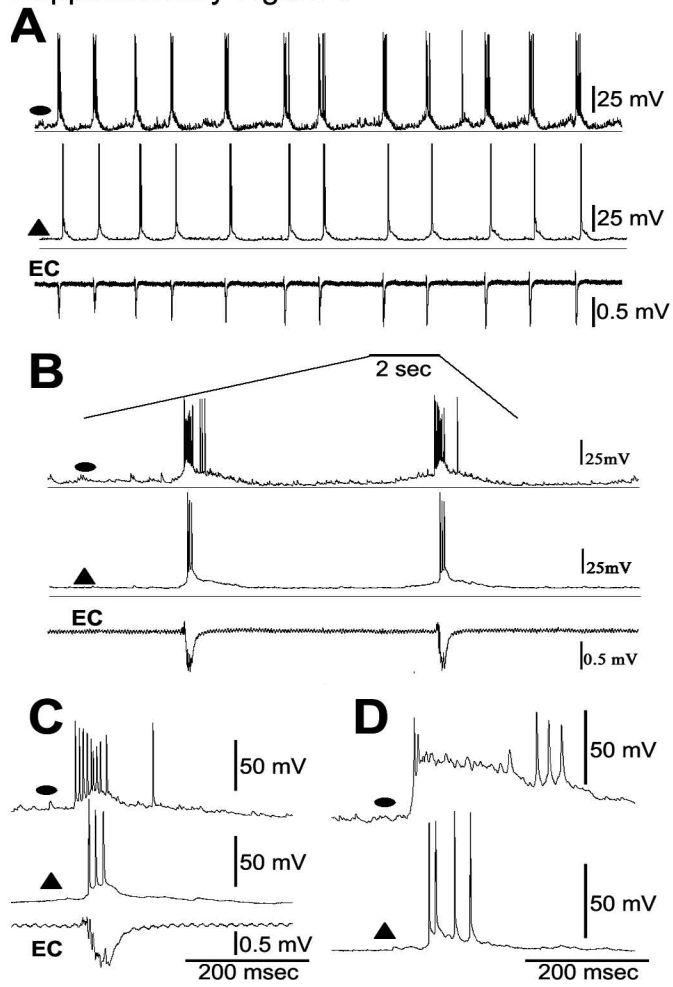
Complete seizure blockade was observed at 20 μ M (n=4). DB returned following a 60-

minute washout. **B.** Traces illustrate seizures recorded in EE pair in isolated CA1. 20 μ M carbenoxolone blocked the seizures, but cells retained sub- and suprathreshold activity.

Dots indicate a time gap in the tracing.

Ziburkus J et al. JN-01378-2005.R2

Supplementary Figure 1



SUPPLEMENTARY FIGURE 2 Ziburkus J et al. JN-01378-2005.R2

